Keywords: layered compounds · silicon · template synthesis · thermochemistry

[1] H. Muranishi, *Bull. Chem. Soc. Jpn.* **1992**, 65, 761 – 770.
[2] A. Crone, K. R. Franklin, P. Graham, *Mater. Chem.* **1995**, *5*, 2007 – 2011.
[3] H. Gies, J. Ruis, *Z. Kristallogr.* **1995**, *210*, 475 – 480.
[4] J. Dewing, M. S. Spencer, T. V. Whittam, *Catal. Rev. Sci. Eng.* **1985**, *27*, 461 – 514.
[5] W. M. Meier, M. Groner, *Solid. Chem.* **1981**, *37*, 204 – 218.
[6] M. E. Davis, R. F. Lobo, *Chem. Mater.* **1992**, *4*, 756 – 768.
[7] U. Oberhagemann, P. Bayat, B. Marler, H. Gies, J. Ruis, *Angew. Chem.* **1996**, *108*, 3041 – 3044; *Angew. Chem. Int. Ed. Engl.* **1996**, *35*, 2869 – 2872.
[8] H. Gies, B. Marler, S. Vortmann, U. Oberhagemann, P. Bayat, K. Krink, J. Rius, I. Wolf, C. Fyfe, *Microporous Mesoporous Mater.* **1998**, *21*, 183 – 197.
[9] S. Hayashi, K. Suzuki, S. Shin, K. Hayamizu, O. Yamamoto, *Chem. Phys. Lett.* **1985**, *113*, 368 – 371.
[10] G. Goor, P. Behrens, J. Felshe, *Microporous. Mater.* **1994**, *2*, 493 – 500.
[11] J. A. Dailey, T. Pinnavaia, *J. Chem. Mater.* **1992**, *4*, 855 – 863
[12] S. Mashimo, N. Mura, T. Uemura, *J. Chem. Phys.* **1992**, *97*, 6759.

Light Harvesting and Energy Transfer in Novel Convergently Constructed Dendrimers**

Sylvain L. Gilat, Alex Adronov, and Jean M. J. Fréchet*

A characteristic of dendritic macromolecules is the presence of numerous peripheral chain ends that all surround a single core.[1] If a long-range interaction could be introduced between these multiple chain ends and the focal point it would then be possible to influence the core of the macromolecule by events that initially occur with a higher probability on the dendrimer periphery.[2] Following this rationale we report that it is possible to essentially create a light-harvesting antenna by functionalizing a dendrimer with suitable interacting chromophores.[3] In these dye-labeled dendrimers light absorbed by the numerous peripheral chromophores is funneled to a central fluorescent core with a remarkably high efficiency and by a mechanism that is independent of the dendritic architecture. Hence, this new strategy is different from all the previous approaches to energy or electron transfer within dendritic architectures,[4] where the transfer was achieved by through-bond or "hopping" processes.

The array of terminal chromophores in the present macromolecules provides a large overall cross-section for collecting energy and plays the role of an antenna for light harvesting, while the focal dye (Figure 1) plays the role of a fluorescent probe whose emission signals that energy is actually received at a single localized site. Furthermore, both the peripheral chromophores and the focal dye contribute to the absorption of the entire macromolecule. Since their individual absorptions each cover a different wavelength range, the absorption of the whole macromolecule is particularly broad and provides a larger spectral coverage than the focal dye alone. The energy transfer process converts this broad absorption into the narrow emission of the central laser dye. Therefore, such a dye-labeled dendrimer represents both a spatial and spectral light concentrator: the energy of any photon of any wavelength absorbed anywhere in this ensemble of chromophores is transferred to a single point and converted into a relatively narrow emission spectrum.

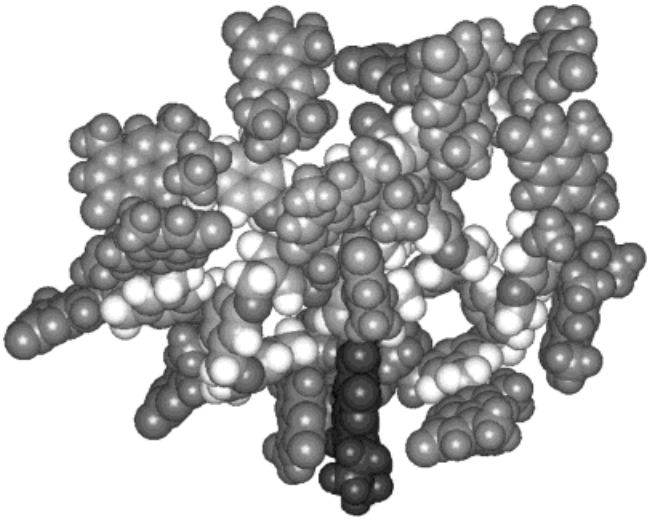

Figure 1. Molecular model (MM3) of the G-4 dendron showing peripheral donor chromophores surrounding the core acceptor (indicated in dark gray).

This scheme is indeed reminiscent of the primary event of photosynthesis, where solar energy absorbed anywhere in an array of hundreds of chlorophyll molecules is efficiently transferred to a single reaction center.[5] The higher the dendrimer generation number, the higher the number of terminal groups that surround the core,[1] and the larger the cross-section for energy collection. However, the average distance between the core and the peripheral groups also increases as the generation number G-x ($x = 1-4$) increases. By considering the size of dendritic macromolecules,[1] energy transfer from the periphery to the core would most likely take place through a dipole – dipole interaction. According to Förster theory[6, 7] the efficiency of energy transfer decreases as the inverse sixth power of the interchromophoric distance. Clearly, it was necessary to determine whether this dipole – dipole interaction would be strong enough to achieve an efficient energy transfer, even at high generations.

[*] Prof. J. M. J. Fréchet, A. Adronov
Department of Chemistry, 718 Latimer Hall
University of California at Berkeley
Berkeley, CA 94720-1460 (USA)
Fax: (+1) 510-643-3079
E-mail: frechet@cchem.berkeley.edu
S. L. Gilat
Bell Laboratories
Murray Hill, NJ 07974 (USA)

[**] This research was supported by the AFOSR MURI program and a Graduate Research Fellowship (A.A.) from the Eastman Kodak Company.

  1433-7851/99/3810-1422 $ 17.50+.50/0

To realize this concept we reviewed carefully the properties of the chromophores currently available from commercial sources.[8] We eventually chose the laser dye coumarin 2 as the donor terminal chromophore, and coumarin 343 as the acceptor focal dye (Scheme 1). A favorable intramolecular charge transfer takes place in the excited state of these

coumarin 2
λ_{max} = 365 nm (20 000)
λ_{em} = 435 nm

coumarin 343
λ_{max} = 446 nm (44 300)
λ_{em} = 490 nm

Scheme 1. Structures and spectral characteristics of the donor and acceptor dyes with extinction coefficients ($L\,mol^{-1}cm^{-1}$) given in parentheses.

molecules, and accounts for their high extinction coefficients and high dipole moments,[8] which are necessary for a strong dipole–dipole interaction. This pair of chromophores meets the basic requirement for energy transfer: the donor emission band strongly overlaps the acceptor absorption band (resonance condition). In addition, the emission of coumarin 2 displays a large Stokes shift, which lowers the probability of self-quenching between the numerous peripheral chromophores. Furthermore, because of their high fluorescence quantum yields and their solubility—a decisive advantage for building multichromophoric macromolecules—these coumarins are used extensively in dye lasers and are therefore commercially available in high purity (> 99 %).

Once the choice of chromophores was secured, a synthetic strategy had to be specifically developed to functionalize the chain ends of a poly(arylether) convergent dendritic backbone by the nucleophilic amino group of coumarin 2, and its focal point by the electrophilic acid functionality of coumarin 343. Since this reactivity polarity is reversed relative to the "classical" convergent synthesis of poly(arylether) dendrimers originally reported by Hawker and Fréchet,[9] the distribution of reactive groups on the dendron, and hence the monomer, had to be inverted so that the same efficient coupling reactions could still be employed. Therefore, the AB_2 monomer used for the building of the "reversed" dendritic structure was a hexadecanesulfonate protected 3,5-bis(bromomethyl)phenol (**1**, Scheme 2),[10] instead of the commonly employed 3,5-dihydroxybenzyl alcohol. The synthetic strategy for the preparation of the dye-labeled poly(arylether) dendrons[11] of generation 1 to 4 began with the nucleophilic attack of two coumarin 2 dyes on the benzyl bromide functionalities of the protected monomer. The resulting dye-labeled fragment was then deprotected with sodium hydroxide in refluxing absolute ethanol to yield the phenol **2**. This phenol could be coupled to coumarin 343 with *N*′-(3-dimethylaminopropyl)-*N*-ethylcarbodiimide (EDC) and 4-dimethylaminopyridine (DMAP) in CH_2Cl_2 to produce the fully dye-labeled first generation dendron **3**. The G-1 phenol **2** was coupled to the AB_2 monomer by the convergent strategy of dendrimer synthesis[9] to yield the second generation protected fragment, which now contained four coumarin 2 dyes. The deprotection and coupling steps were repeated to obtain the G-2 **4** and G-3 **5** dendrons functionalized with both coumarin 2 and coumarin 343 (Scheme 3). The fourth generation fragment was deprotected using sodium ethoxide in DMF. The coupling of the fourth generation phenol to coumarin 343 produced the fully dye-labeled G-4 macromolecule **6**. This synthetic strategy also gives access to model compounds that possess the same arylether backbone but lack either the acceptor dye at the focal point (**7**), or the donor chromophores at the periphery (**8**). The purity of all compounds was carefully monitored by NMR spectroscopy and by matrix-assisted laser desorption/ionization time-of-flight (MALDI-TOF) spectrometry (Figure 2), with special attention being paid to the complete functionalization of the dye-labeled dendrons.

The optical properties of each interactive component were investigated using the model compounds **7** and **8**.[7] As expected the emission band of the donor moiety strongly overlaps the absorption band of the acceptor fragment, thus enabling a highly efficient energy transfer (Figure 3). Moreover, the high probability of heterotransfer over homotransfer can be visualized by comparing this large spectral overlap (gray) to the very weak overlap of the absorption and the emission bands of the donor moiety (black). Whereas the former represents energy transfer to the focal dye, the latter is associated with competitive self-quenching between the terminal chromophores.

Figure 3 also shows that the absorption maximum of each donor or acceptor fragment corresponds exactly to a low minimum for the complementary moiety. It is therefore possible to selectively excite either the donor chromophores or the acceptor dye, which ensures the reliability of the energy transfer results and considerably simplifies analysis of the data. Most importantly, a transfer of energy through the dendritic backbone can be safely ruled out since the poly(arylether) structure itself does not absorb beyond 310 nm: indeed, there is no energy band gap within the internal dendritic framework that is small enough to match the energy of donor emission (418 nm) or the energy of the incoming photons under irradiation at wavelengths $\geq \lambda_{max}$ of the peripheral chromophores (343 nm).

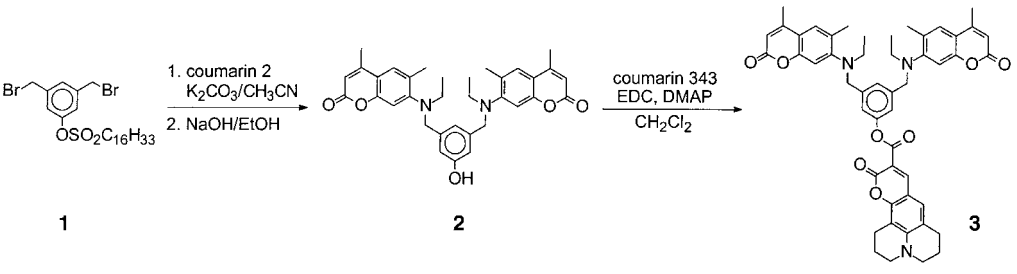

Scheme 2. Synthesis of the fully dye-labeled G-1 dendron.

The absorption of the whole macromolecule at each generation was found

  1433-7851/99/3810-1423 $ 17.50+.50/0

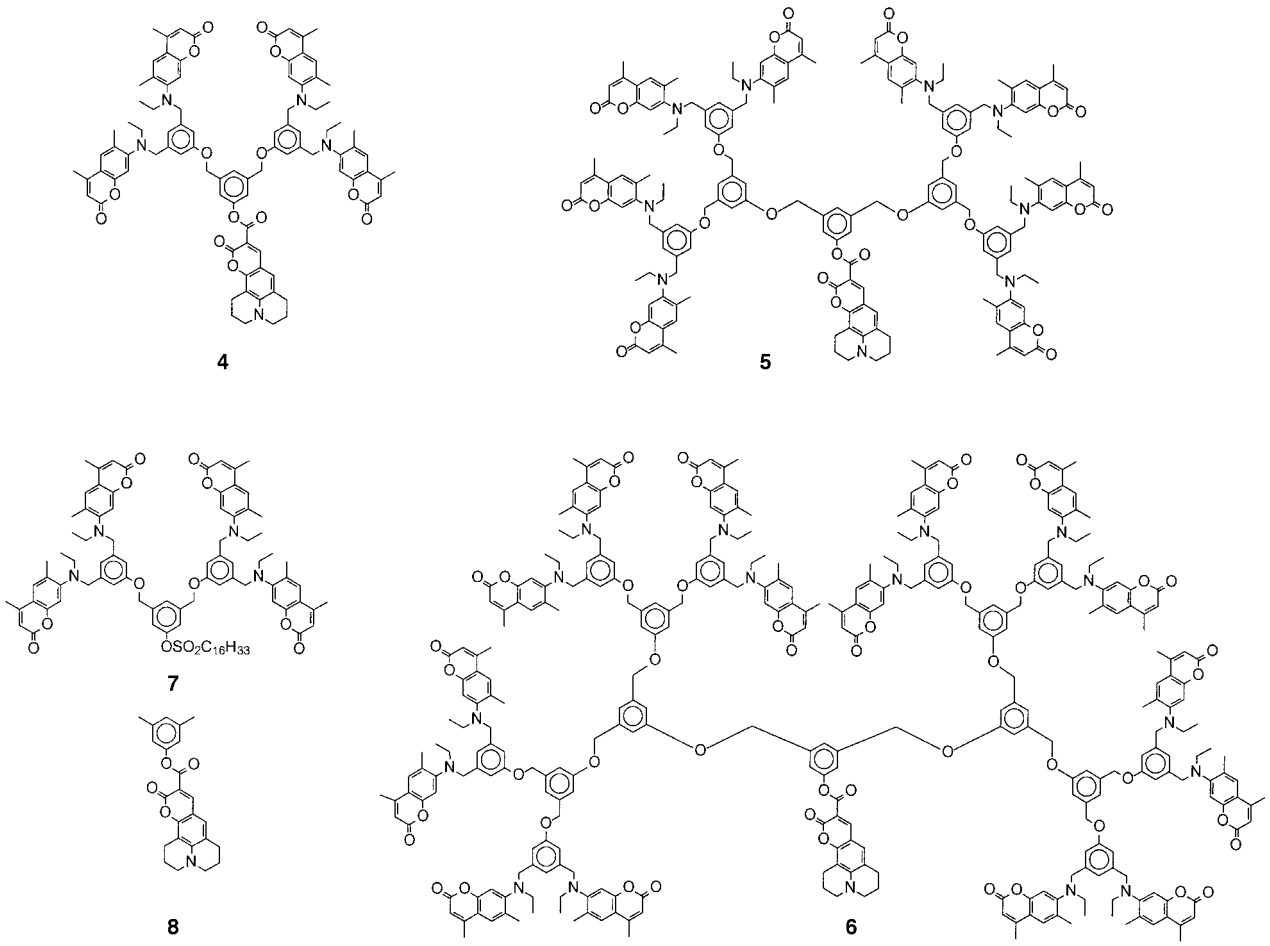

Scheme 3. Structures of the G-2 **4**, G-3 **5**, and G-4 **6** dye-labeled dendrimers as well as the model donor **7** and model acceptor **8** compounds.

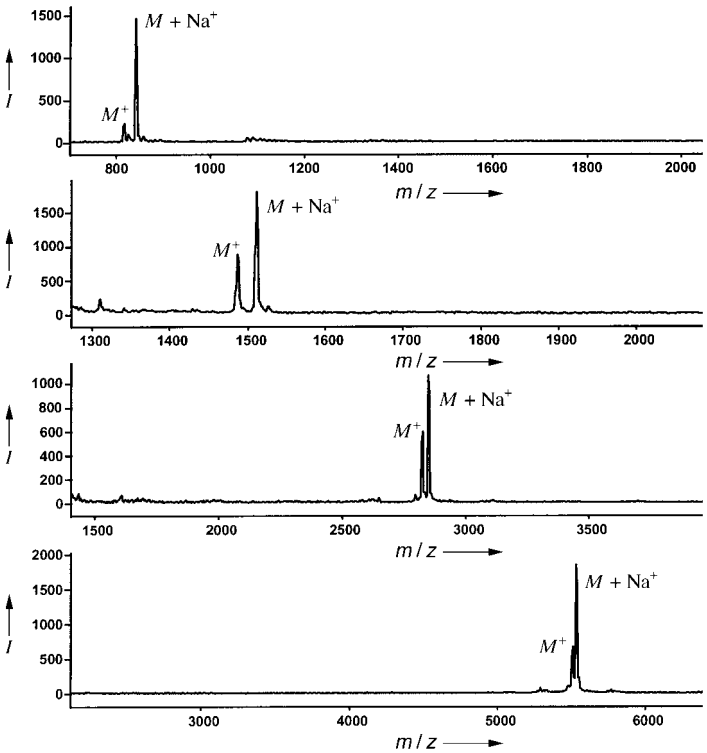

Figure 2. MALDI-TOF mass spectra of the G-1 to G-4 dye-labeled dendrimers **3**–**6** (from top to bottom, respectively).

to closely match the sum of the contributions of each of its individual fragments. This not only confirms the validity of the models, but also demonstrates that there is no interaction in the ground state between the two kinds of laser dye within the same dendron. Consequently, the absorption capacity of the dendrimer increases as a function of the number of terminal chromophores, and the light-harvesting antenna becomes more and more effective as the dendrimer generation increases.

The capacity to focus the energy absorbed by the peripheral antenna of the dendrimer to the central dye is demonstrated in Figure 4 for the G-3 dendron. Excitation of the terminal chromophores at 343 nm is followed by efficient energy transfer to the core and results mainly in the fluorescence at 470 nm (band b) of the focal dye alone. In contrast, excitation of the same peripheral chromophores in the G-3 model compound that lacks the acceptor focal dye results in their single emission at 418 nm (as illustrated in Figure 3 for the G-2 model donor compound). Therefore, the central coumarin functions as a "sink" or spatial energy concentrator that drains energy from the dendrimer periphery. The low intensity of fluorescence at the emission maximum λ_{em} of the peripheral dyes (Figure 4, band a) indicates that fluorescence quenching is remarkably efficient, whereas emission from the central chromophore (band b) demonstrates that the quenched energy is actually received on a localized site and

  1433-7851/99/3810-1424 $ 17.50+.50/0

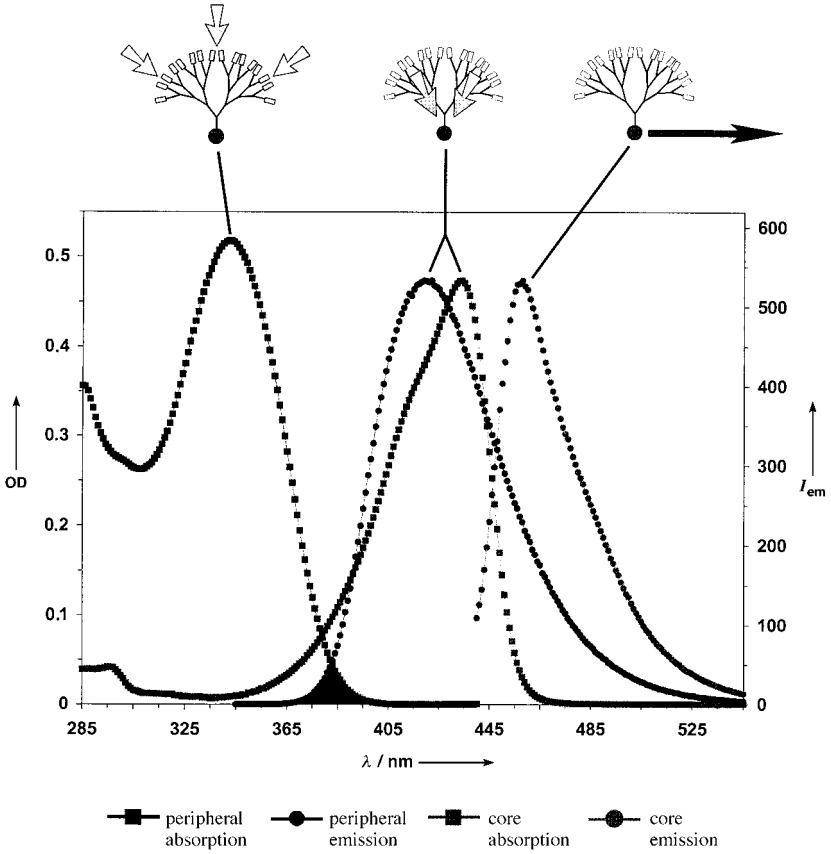

Figure 3. Absorption and emission spectra of the G-2 model donor and acceptor fragments in toluene. Spectral overlaps for heterotransfer and homotransfer are shaded in gray and black, respectively.

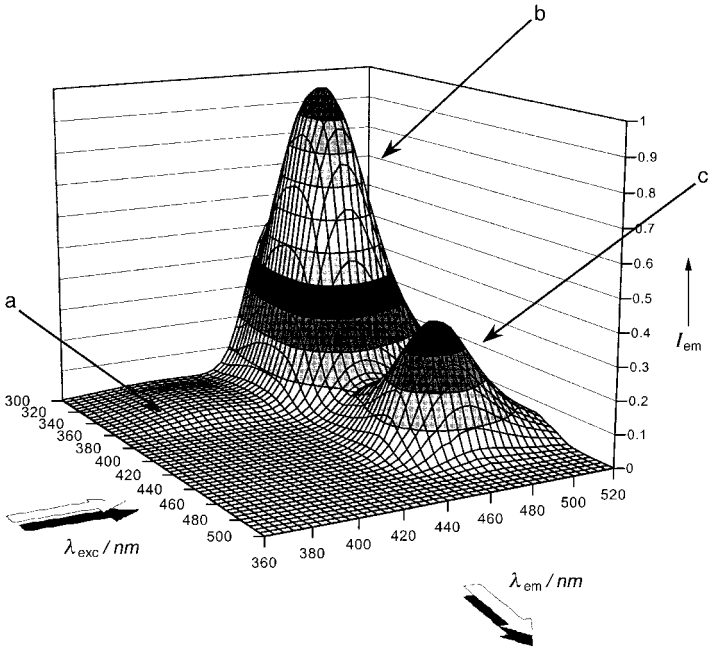

Figure 4. Total fluorescence of the G-3 dendron ($c = 1.17 \times 10^{-6}$ M). a) Spontaneous emission from the peripheral dyes; b) emission from the core dye after energy transfer from the peripheral chromophores; c) emission from the core dye upon direct excitation. All emission spectra have been corrected for slight variations in excitation intensity by dividing out the relative lamp output at each excitation wavelength.

used to excite the focal dye, instead of being dissipated nonradiatively.

The energy transfer efficiency for any given generation of the fully labeled dendrons can be determined in several ways.[7a] One method involves comparing the absorption spectrum with the fluorescence excitation spectrum recorded at the λ_{em} of the focal chromophore. When these two spectra are normalized at the λ_{max} value of the central dye the decrease in intensity at the λ_{max} of the peripheral chromophores in the excitation spectrum relative to the absorption spectrum represents the energy lost in the transfer step.[12] The similarity between the two normalized spectra for G-1 to G-3 is remarkable, and attests to a very high transfer efficiency (close to 100%). The efficiency starts to decrease in G-4 when the donors are excited at their λ_{max} values, as shown in the emission spectrum by some spontaneous fluorescence from these peripheral dyes.[11] A more quantitative analysis of energy transfer efficiency involves the study of the fluorescence quenching of the donor dyes by the acceptor.[7a] Indeed, the fluorescence intensity of the donor dyes in the presence of the acceptor was found to diminish by more than 40-fold in the first three generations, which indicates an energy transfer efficiency of greater than 97%. In the fourth generation the quenching was slightly less effective, and the energy transfer efficiency was found to decrease to 86%. Hence, the synthesized molecules display efficient energy transfer up to the fourth generation.

Figure 4 clearly demonstrates the concept of a spectral energy concentrator. Almost all of the absorbed energy is used to excite the focal dye regardless of the irradiation wavelength, and is eventually converted into its single emission spectrum. In addition, at high generations (G-3 and G-4) the spatial concentration of energy in these molecules results in a net fluorescence amplification when the direct to sensitized excitation of the focal dye are compared (see bands b and c in Figure 4). Since the fluorescence quantum yield of the central dye is large, the whole macromolecule appears to be an effective optical device with excellent absorption and emission features and very few energy losses.

We believe that our approach to energy transfer provides unprecedented flexibility since any dendritic architecture can, in principle, be used to build this type of photoactive device. Not only does this system take advantage of the specific properties of dendritic polymers (high solubility, processability, exact characterization, and well defined structure) in the design of multichromophoric arrays, but the ability to choose the dendritic framework provides versatility for the introduction of an additional key property, such as affinity towards a cell, a protein, or a drug, specific viscosity, specific glass transition, and electron/hole transport capacity. Moreover,

  1433-7851/99/3810-1425 $ 17.50+.50/0

any pair of chromophores can be employed as long as they meet the requirements for mutual interaction. As a result, the emission wavelength of the device can in principle be set in the entire visible range, which is a key property for the design of light emitting materials. Therefore, such dye-labeled dendrimers are promising candidates for a variety of applications, which range, for example, from catalysis (cleavage and release of a photoactive drug or degradation of a photosensitive toxic substance) to amplification for display or mapping, low threshold stimulated emission,[13] solar energy collection, spectral and spatial refocusing of light in fiber optics coatings, and organic optical media.

Experimental Section

Absorption spectra ($OD_{max} < 0.1$) were recorded in toluene (unless otherwise noted) on a Uvicon 933 spectrophotometer. Extinction coefficients were calculated from the Beer–Lambert law, which is followed by all compounds up to an optical density of at least 0.6. The same samples and cells (1 cm) were used to record the emission and excitation spectra directly on an ISA/SPEX Fluorolog 3.22 equipped with a 450 W Xe lamp, double excitation and double emission monochromators, and a digital photon-counting photomultiplier. Slit widths were set to 1.3 nm bandpass on both excitation and emission. Correction for variations in lamp intensity over time and wavelength was achieved with a solid-state silicon photodiode as the reference. The spectra were further corrected for variations in photomultiplier response over wavelength and for the path difference between the sample and the reference by multiplication with emission and excitation correction curves generated on the instrument. The photostability of the dye-labeled dendrons was ascertained by monitoring the emission intensity of the central dye under irradiation at the λ_{max} of the peripheral chromophores: no photodegradation could be detected after 1 h of irradiation. Mass spectra were measured by MALDI-TOF on a Perseptive Biosystems Voyager-DE spectrometer in delayed extraction mode and with an acceleration voltage of 20 keV. Samples were prepared by using a 1:20 ratio of analyte (5 mg mL^{-1} in THF) to matrix solution (*trans*-indoleacrylic acid, 10 mg mL^{-1} in THF).

Synthesis of G-1 **3**: A mixture of **1** (0.590 g, 1.04×10^{-3} mol), coumarin 2 (0.674 g, 3.10×10^{-3} mol, 3 equiv), and K_2CO_3 (0.576 g, 5.43×10^{-3} mol, 5 equiv) was dissolved in dry acetonitrile (27 mL) and stirred at reflux under argon for 72 h. The mixture was then cooled, filtered, and evaporated to dryness in vacuo. The product was purified by chromatography on silica gel using hexanes:ethyl acetate (8:2) as the eluent (yield: 582 mg, 67 %). Deprotection of this G-1 fragment (0.475 g, 5.65×10^{-4} mol) was accomplished by stirring it in refluxing ethanol (200 mL) containing 10 equiv of NaOH for 3 hours. The deprotected product, $(C2)_2$-[G-1]-OH, was isolated by chromatography on silica gel using CH_2Cl_2:ethyl acetate (8:2) as the eluent (82 %). The fully dye-labeled G-1[11] molecule was synthesized by mixing the deprotected phenol **2** (0.100 g, 1.81×10^{-4} mol) with coumarin 343 (0.103 mg, 3.62×10^{-4} mol, 2 equiv), EDC (0.086 g, 4.53×10^{-4} mol, 2.5 equiv), and DMAP (0.005 g, 3.62×10^{-5} mol, 0.2 equiv) in CH_2Cl_2 and stirring the mixture under argon at room temperature overnight (93 %).

The higher generation dendrimers[12] were synthesized by subsequently coupling phenol **2** with the monomer **1**, then deprotecting, and coupling either to coumarin 343 (to obtain the fully labeled dendron) or to the monomer (to go to the next generation). Note that deprotection of G-4 was done in DMF rather than ethanol.

3: ^{1}H NMR (300 MHz, $CDCl_3$, TMS): $\delta = 0.99$ (t, $J = 7.0$ Hz, 6H), 1.96 (m, 4H), 2.34 (s, 6H), 2.36 (d, $J = 1.0$ Hz, 6H), 2.75 (t, $J = 6.1$ Hz, 2H), 2.87 (t, $J = 6.3$ Hz, 2H), 2.99 (q, $J = 7.0$ Hz, 4H), 3.33 (q, $J = 6.1$ Hz, 4H), 4.14 (s, 4H), 6.10 (q, $J = 1.0$ Hz, 2H), 6.68 (s, 2H), 6.97 (s, 1H), 7.03 (s, 2H), 7.13 (s, 1H), 7.33 (s, 2H), 8.47 (s, 1H); ^{13}C NMR (100 MHz, $CDCl_3$): $\delta = 11.82$, 18.56, 18.72, 20.05, 21.11, 27.41, 46.23, 49.97, 50.36, 56.57, 105.75, 107.67, 109.10, 112.54, 114.81, 119.47, 120.46, 124.91, 126.60, 127.33, 129.51, 139.87, 149.11, 150.12, 151.22, 152.43, 152.65, 153.70, 158.50, 161.59, 162.80; MS (MALDI): m/z: 818.53 [M^+], 842.03 [M+Na$^+$], calcd: 819.95, 842.94; UV/Vis (toluene): λ_{max} (ε) = 343 (25 000), 437 nm (45 000).

4: ^{1}H NMR (300 MHz, $CDCl_3$, TMS): $\delta = 1.01$ (t, $J = 7.0$ Hz, 12H), 1.99 (m, 4H), 2.37 (s, 24H), 2.78 (t, $J = 6.1$ Hz, 2H), 2.90 (t, $J = 6.4$ Hz, 2H), 3.00 (q, $J = 7.0$ Hz, 8H), 3.36 (q, $J = 6.4$ Hz, 4H), 4.13 (s, 8H), 3.84 (s, 4H), 6.10 (s, 4H), 6.80 (s, 4H), 6.86 (s, 2H), 6.88 (s, 4H) 6.98 (s, 1H), 7.26 (s, 2H), 7.31 (s, 1H), 7.35 (s, 4H), 8.48 (s, 1H); ^{13}C NMR (100 MHz, $CDCl_3$): $\delta = 11.86$, 14.10, 18.56, 18.71, 20.03, 21.07, 22.63, 25.26, 25.59, 27.39, 31.57, 34.64, 46.25, 49.97, 50.35, 56.62, 67.95, 69.29, 105.61, 105.74, 107.63, 108.99, 112.45, 113.16, 114.66, 119.49, 120.43, 126.55, 127.33, 129.36, 138.78, 139.94, 149.15, 150.08, 151.34, 152.42, 152.61, 153.74, 158.90, 161.56, 162.70; MS (MALDI): m/z: 1486.61 [M^+], 1510.88 [M+Na$^+$], calcd: 1490.75, 1513.74; UV/Vis (toluene): λ_{max} (ε) = 343 (45 000), 438 nm (40 000).

5: ^{1}H NMR (300 MHz, $CDCl_3$, TMS): $\delta = 0.99$ (t, $^3J = 7.0$ Hz, 24H), 1.96 (m, 4H), 2.34 (s, 48H), 2.75 (t, $J = 6.1$ Hz, 2H), 2.87 (t, $J = 6.3$ Hz, 2H), 2.99 (q, $J = 7.0$ Hz, 16H), 3.33 (m, 4H), 4.12 (s, 16H), 4.95 (s, 8H), 5.06 (s, 4H), 6.08 (q, $J = 1.2$ Hz, 8H), 6.80 (s, 8H), 6.85 (s, 4H), 6.86 (s, 8H), 6.93 (s, 1H), 6.99 (s, 4H), 7.06 (s, 2H), 7.30 (s, 2H), 7.32 (s, 9H), 8.44 (s, 1H); ^{13}C NMR (100 MHz, $CDCl_3$): $\delta = 11.84$, 18.53, 18.67, 20.01, 20.04, 21.03, 25.57, 27.37, 35.38, 46.22, 49.92, 50.32, 56.59, 67.94, 69.35, 69.66, 105.42, 105.67, 107.53, 108.95, 112.42, 113.16, 113.30, 114.64, 118.97, 119.48, 120.37, 122.96, 126.53, 127.27, 129.30, 138.64, 138.90, 139.90, 149.16, 150.01, 151.40, 152.39, 152.58, 153.71, 158.34, 158.95, 159.09, 161.49, 162.73; MS (MALDI): m/z: 2828.37 [M^+], 2852.23 [M+Na$^+$], calcd: 2832.37, 2855.35; UV/Vis (toluene): λ_{max} (ε) = 343 (82 000), 441 nm (39 000).

6: ^{1}H NMR (500 MHz, $CDCl_3$, TMS): $\delta = 0.98$ (t, $J = 7.5$ Hz, 48H), 1.93 (m, 4H), 2.32 (s, 96H), 2.70 (m, 2H), 2.81 (m, 2H), 2.98 (q, $J = 7$ Hz, 32H), 3.33 (m, 4H), 4.10 (s, 32H), 4.94 (s, 16H), 5.02 (s, 8H), 5.09 (s, 4H), 6.05 (s, 16H), 6.78 (s, 16H), 6.84 (s, 24H), 7.00 (s, 8H), 7.05 (s, 4H), 7.06 (s, 4H), 7.12 (s, 2H), 7.31 (s, 16H), 8.44 (s, 1H); ^{13}C NMR (125 MHz, $CDCl_3$): $\delta = 11.86$, 18.52, 18.68, 25.59, 46.24, 56.53, 67.96, 69.69, 108.91, 112.41, 113.15, 113.33, 114.62, 120.37, 126.54, 129.26, 138.73, 138.86, 139.89, 152.38, 152.57, 153.69, 158.95, 159.18, 161.45; MS (MALDI): m/z: 5515.05 [M^+], 5534.46 [M+Na$^+$], calcd: 5515.59, 5538.58; UV/Vis (toluene): λ_{max} (ε) = 344 (152 000), 442 nm (38 000).

Received: November 4, 1998 [Z12615IE]
German version: *Angew. Chem.* **1999**, *111*, 1519–1524

Keywords: chromophores · dendrimers · energy transfer · light harvesting · molecular devices

[1] a) D. A. Tomalia, A. M. Naylor, W. A. Goddard III, *Angew. Chem.* **1990**, *102*, 119–157; *Angew. Chem. Int. Ed. Engl.* **1990**, *29*, 138–175; b) J. M. J. Fréchet, *Science* **1994**, *263*, 1710–1715; c) J. M. J. Fréchet, C. J. Hawker in *Synthesis and Properties of Dendrimers and Hyperbranched Polymers*, *Comprehensive Polym. Sci., 2nd Suppl.* (Eds.: S. L. Aggarwal, S. Russo), Pergamon, Oxford, **1996**, p. 140; d) G. R. Newkome, C. N. Moorefield, F. Vogtle, *Dendritic Molecules: Concepts*, *Syntheses*, *Perspectives*, VCH, Weinheim, **1996.**

[2] a) A. Bar-Haim, J. Klafter, R. Kopelman, *J. Am. Chem. Soc.* **1997**, *119*, 6197–6198; b) A. Bar-Haim, J. Klafter, *J. Phys. Chem. B* **1998**, *102*, 1662–1664.

[3] a) D. Ng, J. E. Guillet, *Macromolecules* **1982**, *15*, 724–727; b) L. Jullien, J. Canceill, B. Valeur, E. Bardez, J.-M. Lehn, *Angew. Chem.* **1994**, *106*, 2582–2584; *Angew. Chem. Int. Ed. Engl.* **1994**, *33*, 2438–2439; c) L. Jullien, J. Canceill, B. Valeur, E. Bardez, J.-P. Lefèvre, J.-M. Lehn, V. Marchi-Artzner, R. Pansu, *J. Am. Chem. Soc.* **1996**, *118*, 5432–5442; d) J. Seth, V. Palaniappan, T. E. Johnson, S. Prathapan, J. S. Lindsey, D. F. Bocian, *J. Am. Chem. Soc.* **1994**, *116*, 10578–10592; e) J.-S. Hsiao, B. P. Krueger, R. W. Wagner, T. E. Johnson, J. K. Delaney, D. C. Mauzerall, G. R. Fleming, J. S. Lindsey, D. F. Bocian, R. J. Donohoe, *J. Am. Chem. Soc.* **1996**, *118*, 11181–11193; M. S. Vollmer, F. Würthner, F. Effenberger, P. Emele, D. U. Meyer, T. Stümpfig, H. Port, H. C. Wolf, *Chem. Eur. J.* **1998**, *4*, 260–269.

[4] a) G. Denti, S. Campagna, S. Serroni, M. Ciano, V. Balzani, *J. Am. Chem. Soc.* **1992**, *114*, 2944–2950; b) P. Belser, A. von Zelewsky, M. Frank, C. Seel, F. Vögtle, L. De Cola, F. Barigelletti, V. Balzani, *J. Am. Chem. Soc.* **1993**, *115*, 4076–4086; c) V. Balzani, S. Campagna, G. Denti, A. Juris, S. Serroni, M. Venturi, *Acc. Chem. Res.* **1998**, *31*, 26–34; d) Z. Xu, J. S. Moore, *Acta Polymer.* **1994**, *45*, 83–87; e) C.

  1433-7851/99/3810-1426 $ 17.50+.50/0

Devadoss, P. Bharati, J. S. Moore, *J. Am. Chem. Soc.* **1996**, *118*, 9635 – 9644; f) P.-W. Wang, Y.-J. Liu, C. Devadoss, P. Bharathi, J. S. Moore, *Adv. Mater.* **1996**, *3*, 237 – 241; g) G. M. Stewart, M. A. Fox, *J. Am. Chem. Soc.* **1996**, *118*, 4354 – 4360.

[5] a) G. McDermott, S. M. Prince, A. A. Freer, A. M. Hawthornthwaite-Lawless, M. Z. Papiz, R. J. Cogdell, N. W. Isaacs, *Nature* **1995**, *374*, 517 – 521; b) W. Kühlbrandt, *Nature* **1995**, *374*, 497 – 498.

[6] a) T. Förster, *Z. Naturforsch. A* **1949**, *4*, 319 – 327; b) T. Förster, *Discuss. Faraday Soc.* **1959**, *27*, 7 – 17; c) L. Stryer, *Ann. Rev. Biochem.* **1978**, *47*, 819 – 846; d) B. Wieb Van Der Meer, G. Coker III, S.-Y. Simon Chen, *Resonance Energy Transfer*, *Theory and Data*, VCH, Weinheim, **1994**.

[7] a) J. Bourson, J. Mugnier, B. Valeur, *Chem. Phys. Lett.* **1982**, *92*, 430 – 432; b) J. Mugnier, J. Pouget, J. Bourson, B. Valeur, *J. Lumin.* **1985**, *33*, 273 – 300; c) B. Valeur in *Fluorescent Biomolecules*, *Methodologies and Applications* (Eds.: D. M. Jameson, G. D. Reinhart), Plenum, New York, **1989**, pp. 269 – 303; d) B. Valeur in *Molecular Luminescence Spectroscopy*, *Part 3*, *Vol. 77* (Ed.: S. G. Schulman), Wiley, New York, **1993**, chap. 2.

[8] For the optical properties of commercial dyes see the Kodak or Molecular Probes catalogs.

[9] a) C. J. Hawker, J. M. J. Fréchet, *J. Chem. Soc. Chem. Commun.* **1990**, 1010 – 1013; b) C. J. Hawker, J. M. J. Fréchet, *J. Am. Chem. Soc.* **1990**, *112*, 7638 – 7647.

[10] T. L. Tyler, J. E. Hanson, *Polym. Mater. Sci. Eng.* **1995**, *73*, 356 – 357.

[11] Synthesis, detailed characterization, and quantitative photophysical characteristics of these molecules will be described shortly: S. L. Gilat, A. Adronov, J. M. J. Fréchet, unpublished results.

[12] L. Stryer, R. P. Haugland, *Proc. Natl. Acad. Sci. USA* **1967**, *58*, 719 – 726.

[13] M. Beggren, A. Dodabalapur, R. E. Slusher, Z. Bao, *Nature* **1997**, *389*, 466 – 469.

The First Direct Synthesis of Corroles from Pyrrole**

Zeev Gross,* Nitsa Galili, and Irena Saltsman

Core-modified porphyrins have been receiving increased attention in recent years,[1] mainly because of their superiority over porphyrins in many applications, most notably as agents for photodynamic therapy.[2] Some of these macrocycles form complexes with transition metals, which due to the alteration of the ligand structure have very different properties than the analogous metalloporphyrins. The most interesting compounds in this regard are corroles, whose skeletons are contracted by one carbon atom with respect to porphyrins (Scheme 1).[3] In contrast to the diprotonic porphyrins, corroles act as tetradentate trianionic ligands toward metal ions. The most remarkable feature of corroles is the stabilization of unusually high oxidation states, such as iron(IV), cobalt(IV), and cobalt(V).[4] Surprisingly, however, there is no reported application in any field for either corroles or their metal complexes. The reason for that is almost certainly the lack of obvious procedures for their preparation. Thus, in spite of the significant progress in corrole synthesis, even the most simple procedures reported to date require starting materials that are not commercially available.[5] Similarly, the first synthesis of a *meso*-substituted corrole—*meso*-aryl substitution is most likely a prerequisite for the utilization of metallocorroles in catalysis—appeared only in 1993.[6]

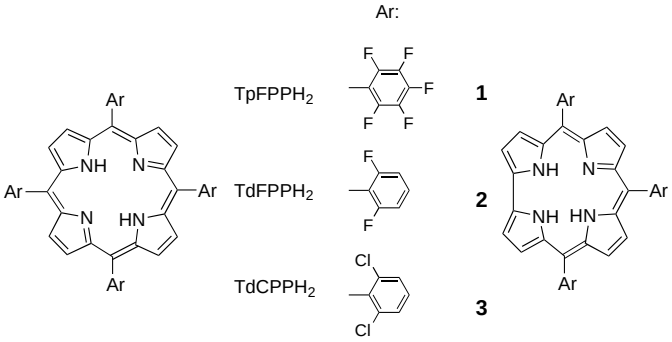

Scheme 1. Schematic representation of tetraarylporphyrins $TpFPPH_2$, $TdFPPH_2$, and $TdCPPH_2$ (left) and the corresponding triarylcorroles **1** – **3** (right).

Owing to our ongoing interest in the synthesis of porphyrins and their core-modified analogues,[7] we explored a new approach, the solvent-free condensation of pyrrole and aldehydes. The research goal was the development of a simple synthetic methodology for the preparation of porphyrins, driven by the anticipation that the rather unusual reaction conditions might also lead to the formation of some porphyrin isomers. We have focused on two aldehydes: benzaldehyde, as the prototype of other *meso*-aryl-substituted porphyrins, and perfluorobenzaldehyde, because the metal complexes of the corresponding porphyrin ($TpFPPH_2$, Scheme 1) are among the most efficient oxygenation catalysts. The reaction conditions were very simple indeed, consisting of mixing pyrrole and the aldehyde in equimolar quantities on a solid support, heating to 100 °C for four hours, oxidation with 2,3-dichloro-5,6-dicyano-1,4-benzoquinone (DDQ), and chromatographic separation. The reaction vessel was open to air, which not only simplifies the procedure but was also found to be required. With benzaldehyde as reactant, tetraphenylporphyrin ($TPPH_2$) was obtained in 5 – 8 % yield, depending on the solid support (see Experimental Section).

When the same reaction conditions (best with basic alumina as solid support) were applied for perfluorobenzaldehyde, very different results were observed. Only traces of the corresponding porphyrin ($TpFPPH_2$) were obtained, accompanied by a compound (**1**, isolated in 11 % yield) which showed a strong porphyrin-like fluorescence and an electronic spectrum similar to that of $TpFPPH_2$ (Figure 1). However, while the ^1H NMR spectrum of $TpFPPH_2$ consists of two singlets in a ratio of 8:2 at $\delta = 8.91$ (sharp) and -2.93 (broad) for the β-pyrrole and the inner nitrogen hydrogen atoms, respectively, in the spectrum of **1** three doublets ($J \approx 4.5$ Hz) in the ratio of 1:1:2 were obtained in the pyrrole hydrogen region ($\delta = 9.10$, 8.75, and 8.57) together with an extremely broad resonance at $\delta = -2.25$ (Figure 1, inset). Similarly, the

[*] Dr. Z. Gross, Dr. N. Galili, Dr. I. Saltsman
Department of Chemistry
Technion – Israel Institute of Technology
Haifa 32000 (Israel)
Fax: (+972) 4-823-3735
E-mail: chr10zg@tx.technion.ac.il

[**] We acknowledge the partial support of this research by The R. and M. Rochlin Research Fund (Z.G.) and The Center for Absorption in Science, Ministry of Immigrant Absorption, State of Israel (I.S.).

  1433-7851/99/3810-1427 $ 17.50+.50/0